

Transparent Quasi-Interdigitated Electrodes for Semi-transparent Perovskite Back-Contact Solar Cells

Giovanni DeLuca, Askhat N. Jumabekov, Yinghong Hu, Alexandr N. Simonov, Jianfeng Lu, Boer Tan, Gede W.P. Adhyaksa, Erik Garnett, Elsa Reichmanis, Anthony Sidney Richard Chesman, and Udo Bach

ACS Appl. Energy Mater., **Just Accepted Manuscript** • DOI: 10.1021/acsaem.8b01140 • Publication Date (Web): 20 Aug 2018

Downloaded from <http://pubs.acs.org> on August 21, 2018

Just Accepted

“Just Accepted” manuscripts have been peer-reviewed and accepted for publication. They are posted online prior to technical editing, formatting for publication and author proofing. The American Chemical Society provides “Just Accepted” as a service to the research community to expedite the dissemination of scientific material as soon as possible after acceptance. “Just Accepted” manuscripts appear in full in PDF format accompanied by an HTML abstract. “Just Accepted” manuscripts have been fully peer reviewed, but should not be considered the official version of record. They are citable by the Digital Object Identifier (DOI®). “Just Accepted” is an optional service offered to authors. Therefore, the “Just Accepted” Web site may not include all articles that will be published in the journal. After a manuscript is technically edited and formatted, it will be removed from the “Just Accepted” Web site and published as an ASAP article. Note that technical editing may introduce minor changes to the manuscript text and/or graphics which could affect content, and all legal disclaimers and ethical guidelines that apply to the journal pertain. ACS cannot be held responsible for errors or consequences arising from the use of information contained in these “Just Accepted” manuscripts.

Transparent Quasi-Interdigitated Electrodes for Semi-transparent Perovskite Back-Contact Solar Cells

*Giovanni DeLuca,^{a,b,c,†} Askhat N. Jumabekov,^{b,††} Yinghong Hu,^{b,d} Alexandr N. Simonov,^{e,f}
Jianfeng Lu,^c Boer Tan,^c Gede W. P. Adhyaksa,^g Erik C. Garnett,^g Elsa Reichmanis,^{a,h*} Anthony
S. R. Chesman,^{b,i*} and Udo Bach^{c,i,j*}*

^a School of Chemistry and Biochemistry, Georgia Institute of Technology, Atlanta, Georgia, 30332, United States

^b CSIRO Manufacturing, Clayton, Victoria, 3168, Australia

^c Department of Chemical Engineering, Monash University, Clayton, 3800, Victoria, Australia

^d Department of Chemistry and Center for NanoScience (CeNS), LMU Munich, 80539, Munich, Germany

^e School of Chemistry, Monash University, Clayton, Victoria, 3800, Australia

^f ARC Centre of Excellence for Electromaterials Science, Monash University, Clayton, Victoria, 3800, Australia

^g Center for Nanophotonics, AMOLF, 1098 XG, Amsterdam, The Netherlands

^h School of Chemical and Biomolecular Engineering, Georgia Institute of Technology, Atlanta, Georgia, 30332, United States

ⁱ Melbourne Centre for Nanofabrication, Clayton, Victoria, 3168, Australia

^j ARC Centre of Excellence for Exciton Science, Monash University, Victoria, 3800, Australia

‡ Contributed equally to this work

* Corresponding authors. E-mail address: udo.bach@monash.edu (U. Bach), elsa.reichmanis@chbe.gatech.edu (E. Reichmanis), anthony.chesman@csiro.au (A. S. R. Chesman).

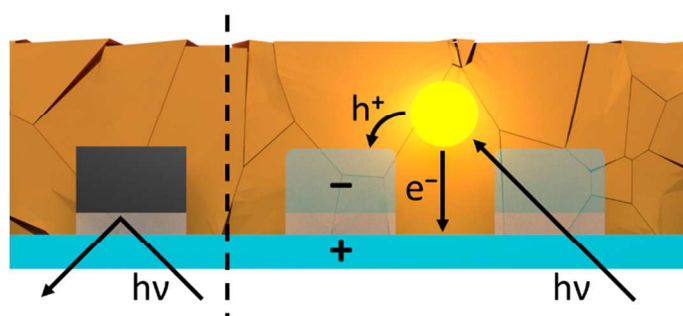
† Present address. Department of Physics, School of Science and Technology, Nazarbayev University, Astana, 010000, Kazakhstan

ORCID:

Anthony Chesman: 0000-0002-1807-4468

Elsa Reichmanis: 0000-0002-8205-8016

Giovanni DeLuca: 0000-0002-3456-1020



Transparent quasi-interdigitated electrodes (t-QIDEs) were produced by replacing the opaque components of existing QIDEs with indium tin oxide (ITO). We demonstrate their application in the first semi-transparent back-contact perovskite solar cell. A device with a V_{OC} of 0.88 V and a J_{SC} of 5.6 mA cm^{-2} produced a modest 1.7% efficiency. The use of ITO allows for illumination of the device from front- and rear-sides, resembling a bifacial solar cell, both of which yield comparable efficiencies. Coupled optoelectronic simulations reveal this architecture may achieve power conversion efficiencies of up to 11.5%, and 13.3% when illuminated from front- and rear-side, respectively, using a realistic quality of perovskite material.

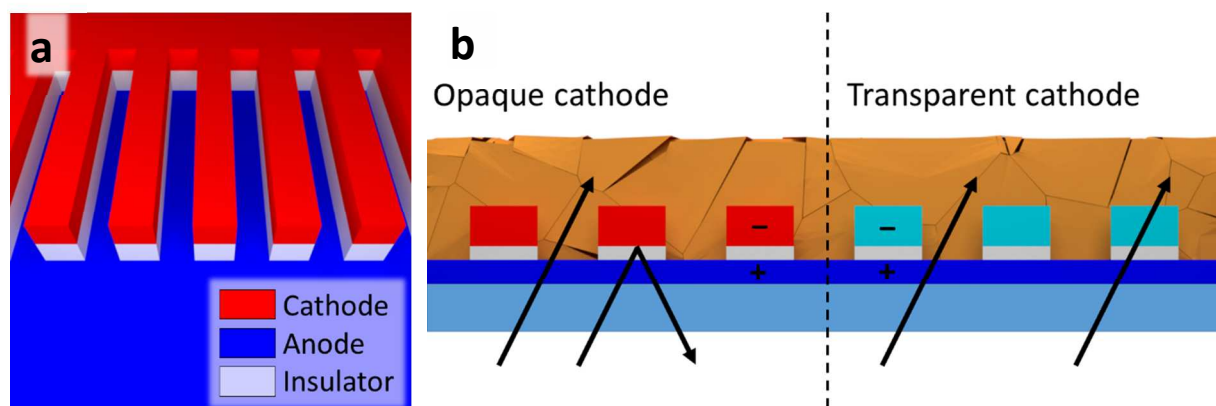
[Keywords]: Back-contact solar cell, perovskite solar cell, coupled optical-electrical modeling, transparent conducting oxides, transparent quasi-interdigitated electrodes

1
2
3 While back-contact electrodes (BCEs) are incorporated into the highest efficiency silicon
4 solar cells,¹ they are yet to be adopted by researchers fabricating organometal halide perovskite
5 analogues. The fabrication of back-contact perovskite solar cells (BC-PSCs) will eliminate
6 parasitic absorption by the top contact, and leave the perovskite surface exposed, allowing for
7 improvements through light-trapping, the application of an anti-reflective coating, new post -
8 annealing techniques, surface passivation, and photoluminescence out-coupling.²⁻³ Furthermore,
9 the architecture offers several functional advantages during fabrication, including the elimination
10 of shorting due to pinholes, and avoiding damage to the perovskite layer during the deposition of
11 subsequent layers.⁴ However, the electrode spacing in the BCEs currently used in Si solar cells is
12 too large for perovskites which have shorter carrier diffusion lengths. Also, the processes used to
13 fabricate commercial BCEs are not compatible with perovskite thin films,⁵ thus prohibiting the
14 direct transfer of existing technology to this new class of photoabsorber material.
15
16
17
18
19
20
21
22
23
24
25
26
27
28
29
30

31 The realization of operational BC-PSCs therefore necessitated the development of a new
32 device architecture, namely quasi-interdigitated electrodes (QIDEs) (Figure 1a). This back-
33 contact architecture places a finger-shaped cathode onto a continuous thin-film anode, with an
34 insulating layer separating the electrodes. This avoids formation of the short-circuit pathways
35 that occur in conventional co-planar interdigitated electrodes when a defect in one electrode
36 finger causes contact with an adjacent electrode, a problem that increases in frequency as the
37 electrode features are miniaturized to the dimensions required for the charge carrier diffusion
38 lengths of perovskites.⁴
39
40
41
42
43
44
45
46
47
48
49

50 Although QIDEs present a robust architecture for BC-PSCs, a key design element limits
51 their potential application. The top contacts are currently comprised of opaque Al/NiCo fingers,
52 which are strong absorbers/reflectors of incident light (Figure 1b), preventing their use in
53
54
55
56
57
58
59
60

1
2
3 semitransparent PSCs or as the top electrode in tandem perovskite-silicon solar cells. Therefore,
4
5 for QIDEs to reach their full potential, the top electrode must be replaced with a transparent
6
7 conductor. To this end, we introduce herein the first transparent quasi-interdigitated electrode (t-
8
9 QIDEs) based on indium tin oxide (ITO), which has a high carrier concentration, low sheet
10
11 resistance, and, most importantly, higher optical transmittance (>85% in visible wavelengths)
12
13 than Al/NiCo.⁶ Furthermore, we demonstrate the first operational semi-transparent back-contact
14
15 perovskite solar cell. Optoelectronic theoretical simulations² also show the realistically
16
17 achievable power conversion efficiencies (PCEs) and average visible transmissions (%AVT)
18
19 with varying perovskite film thicknesses.
20
21
22
23
24
25
26
27



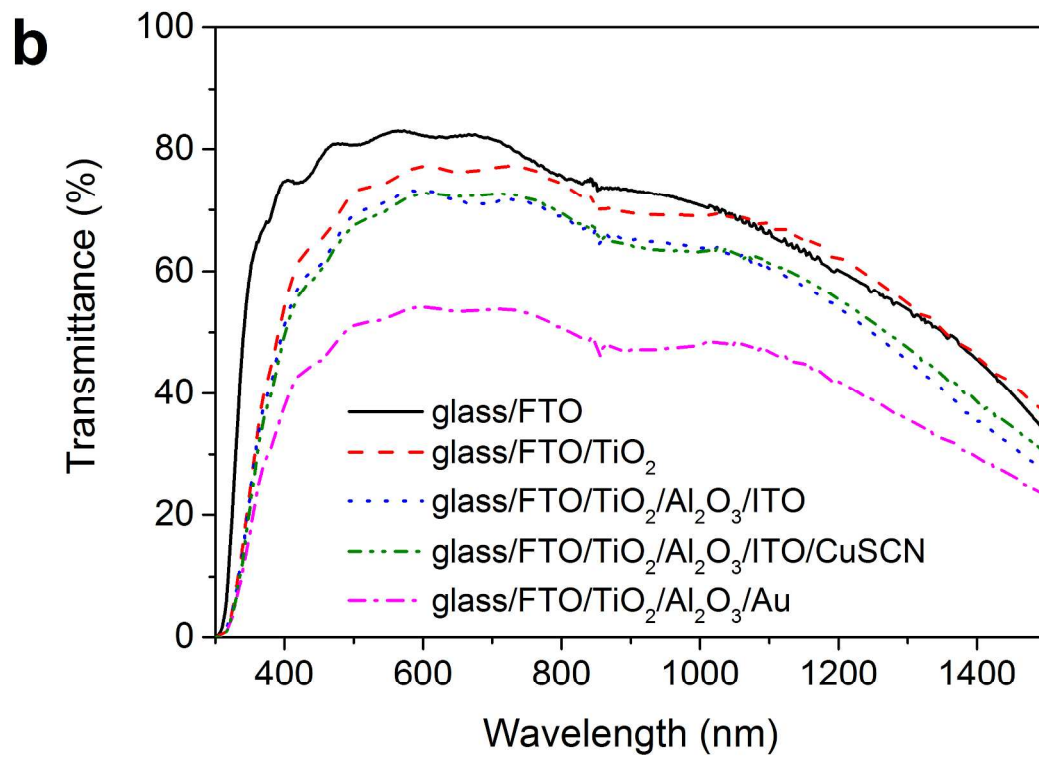
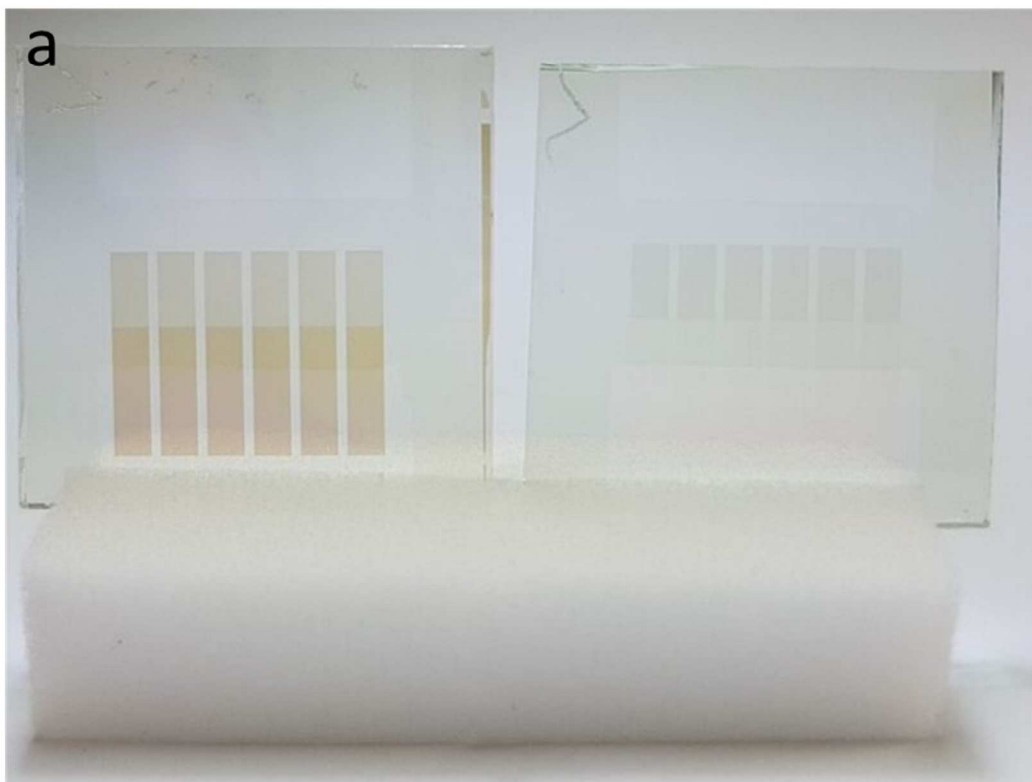
28
29
30
31
32
33
34
35
36
37
38
39
40
41
42 **Figure 1.** (a) The structure of a QIDEs. (b) Light transmission, absorption and reflection in
43 QIDEs with Al/NiCo electrodes (left) or transparent electrodes (right).
44
45
46
47

48 Creating a t-QIDE first required optimization of the deposition of ITO that replaced the
49
50 opaque components in the original architecture. This was achieved by varying the following
51
52 deposition parameters: substrate temperature, ITO target power, argon and oxygen flow rates,
53
54 and post-deposition annealing conditions. The optimized process yielded ~200 nm ITO thin
55
56
57
58
59
60

1
2
3 films with an optical transmittance of ca. 88% at 592 nm (Figure S1), and sheet resistances
4 ranging from 25 to 35 Ω square⁻¹. Photoelectron spectroscopy in air (PESA) measurements
5 confirmed the ITO had a work function (4.78 ± 0.08 eV) comparable to literature values (Figure
6 S2 and Table S1).⁷

7
8
9
10
11
12
13 Post-deposition annealing for 3 minutes at 300 °C was required to enhance transmittance in
14 the solar spectrum region (Figure S1). This accompanied the transformation of fully amorphous
15 ITO to a highly crystalline phase, as evidenced by X-ray diffraction (XRD) measurements
16 (Figure S3). In addition, post-deposition annealing resulted in a twenty-fold decrease in sheet
17 resistance. While heating the substrate during ITO deposition is preferable to post-deposition
18 annealing,⁸⁻⁹ the high temperatures required for the former process are not compatible with the
19 photoresist used during t-QIDEs fabrication, therefore the sample required the post-annealing
20 process.

21
22
23
24
25
26
27
28
29
30
31
32 Once optimized, the deposition parameters were applied to the fabrication of ITO fingers for
33 t-QIDEs. The initial electrode fabrication steps followed previously reported work,⁴ where a
34 photoresist served as the negative of the electrode pattern applied to a TiO₂/FTO stack on glass,
35 followed by the deposition of an Al₂O₃ insulating layer to separate the anode and cathode. A
36 continuous thin film of ITO was then deposited, and subsequent lift-off of the photoresist mask
37 afforded ITO electrode fingers. Images taken following lift-off revealed the mask was
38 completely removed and the ITO fingers were undamaged (Figure S4). After removing the
39 photoresist mask, the electrodes were annealed, transforming the electrodes from light-brown to
40 colorless (Figure 2a). Finally, to ensure the electrodes have the necessary band energy alignment
41 with a perovskite photoabsorber, a suitable hole transport material, copper (I) thiocyanate, was
42 electrodeposited onto the ITO fingers prior to perovskite deposition.

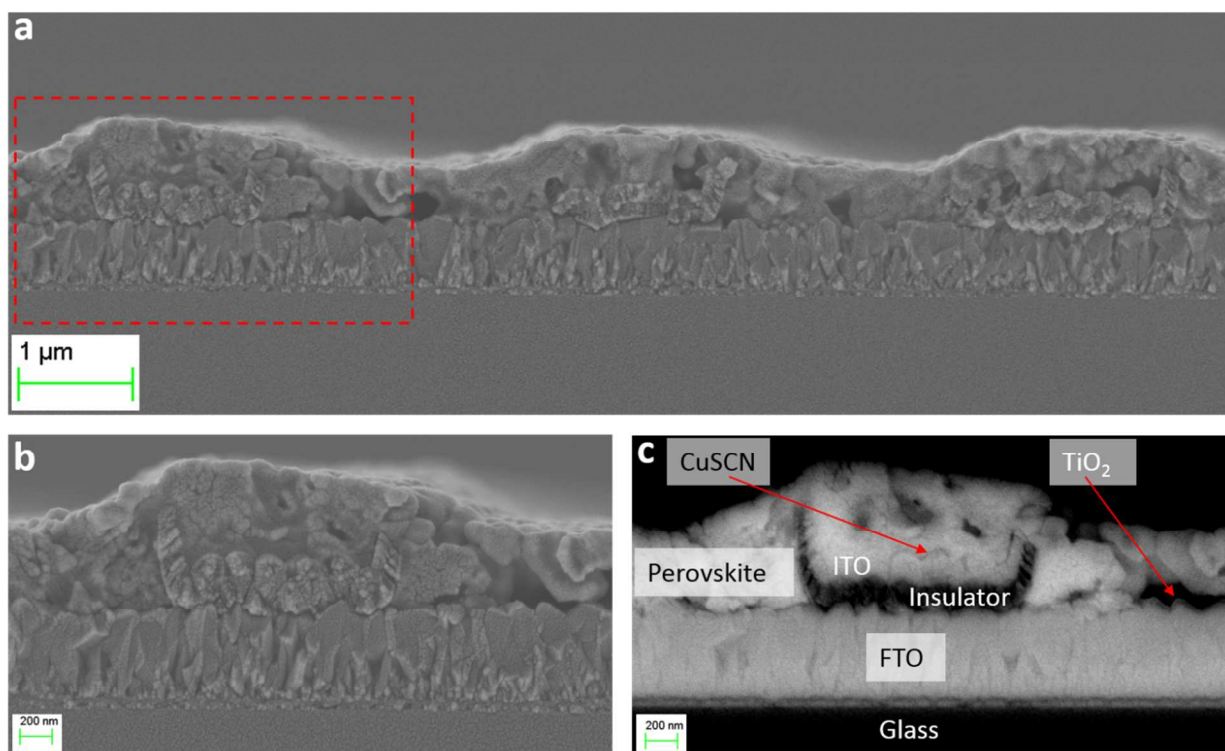


1
2
3 **Figure 2.** (a) Photograph of t-QIDEs before (left) and after annealing at 300 °C (right). (b) UV-
4 Vis-NIR transmission spectra of the t-QIDEs at various stages of fabrication, and for QIDEs with
5 a gold top electrode.
6
7
8

9 UV-Vis-NIR spectroscopy measurements were performed on the electrode stack at each
10 stage of the fabrication process to determine the contribution of each component to the incident
11 light absorption of the t-QIDEs (Figure 2b, Table S2 and Table S3). The pristine FTO-coated
12 glass exhibited the highest transmittance, while TiO₂ deposition resulted in a slight drop in
13 transmittance in the blue and visible regions of the spectrum. After depositing the Al₂O₃/ITO top
14 electrode (quasi-interdigitated area), the overall transmittance decreased by approximately 15%
15 and 10% relative to the FTO glass substrate and FTO/TiO₂ anode, respectively. This results
16 mainly from the formation of additional interfaces (TiO₂/Al₂O₃ and Al₂O₃/ITO), which enhance
17 the reflectance of the electrode assembly. The addition of the hole transport layer caused
18 insignificant changes to the average transmittance (Figure 2b). The t-QIDE architecture is an
19 ordinary reciprocal system that gives identical transmission through both sides, with insignificant
20 differences probably arising from scattering (Figure S5). To demonstrate the transparency of the
21 ITO fingers, identical measurements were performed on a device where ITO was replaced with a
22 *ca.* 60 nm thick layer of gold. This substitution resulted in a significant decrease in transmission
23 to *ca.* 50%, confirming that the relatively high transmittance of the t-QIDEs is due to the
24 transparent nature of ITO (Figure 2b).
25
26
27
28
29
30
31
32
33
34
35
36
37
38
39
40
41
42
43
44
45

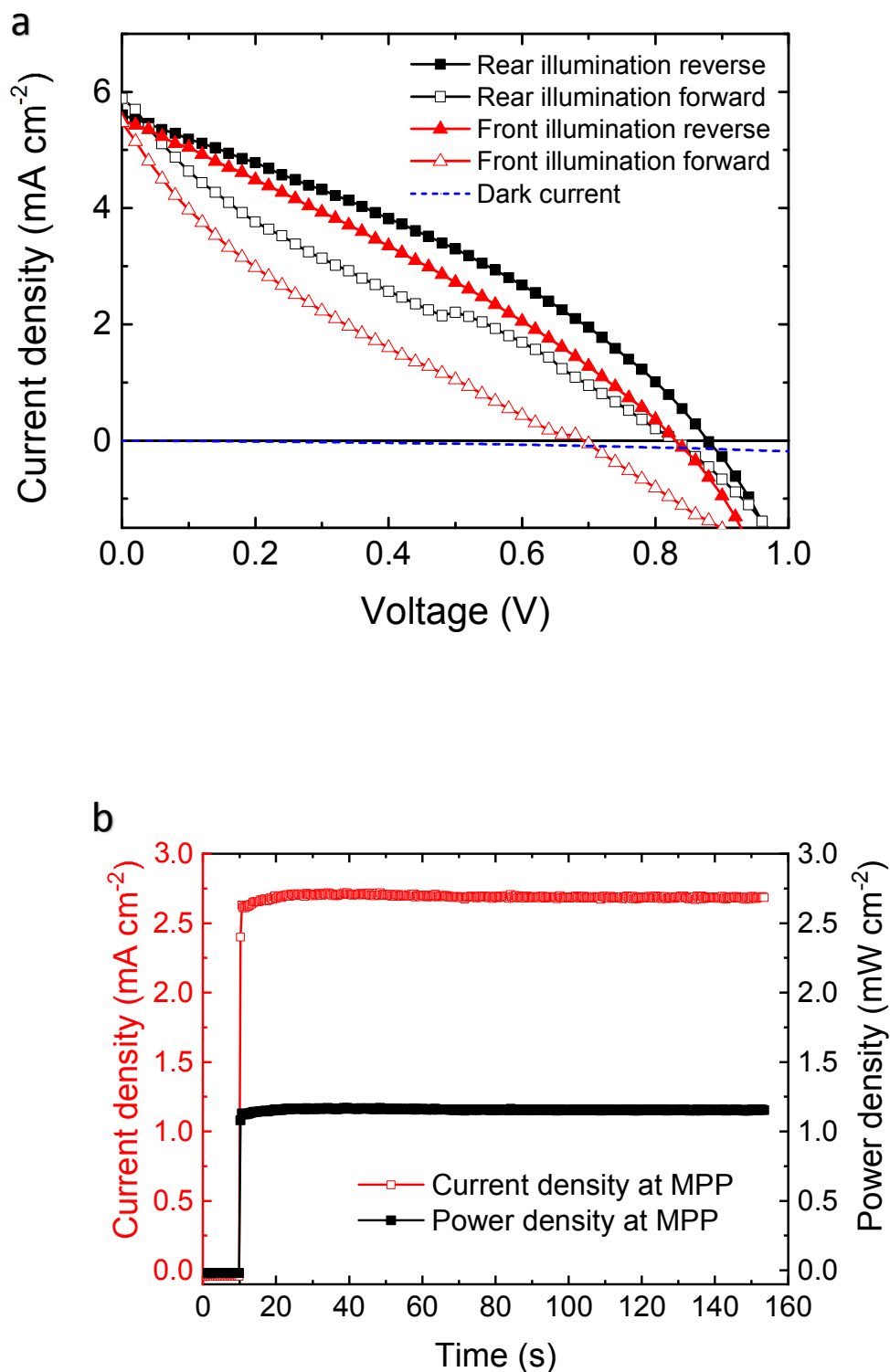
46 While t-QIDEs could potentially be applied to a range of photoabsorber materials, CuSCN
47 was applied to the ITO to provide a band energy alignment compatible with hybrid organic-
48 inorganic perovskites (Figures S6-7). For this study we selected a multiple-cation mixed-halide
49 perovskite with the nominal composition Cs_{0.05}FA_{0.79}MA_{0.16}PbI_{2.49}Br_{0.51} as the photoabsorber,
50 which has shown high photovoltaic efficiencies.¹⁰ Figure 3a presents a cross-sectional scanning
51
52
53
54
55
56
57
58
59
60

1
2
3 electron micrograph of a back-contact PSC based on t-QIDEs. The back-scattered electron image
4 of an individual finger reveals that a thin perovskite layer (~ 340 nm) uniformly covers the t-
5 QIDE, which consists of a micro-structured cathode (~ 1.5 μm wide ITO/CuSCN fingers spaced
6 every ~ 2.5 μm) on a continuous anode (FTO/TiO₂ on glass), separated by ~ 100 nm of Al₂O₃
7 (Figure S8). The micro-fingers of the cathode were trough shaped rather than perfectly flat, due
8 to the polymer mask fabrication process where the edges of the grooves formed by the mask are
9 imperfectly defined. A back-scattered electron cross-section image provides additional contrast
10 to differentiate the functional device layers (Figure 3c).
11
12
13
14
15
16
17
18
19
20
21
22
23
24



49
50 **Figure 3.** (a) Cross-sectional SEM image of the back-contact PSC based on the
51 Cs_{0.05}FA_{0.79}MA_{0.16}PbI_{2.49}Br_{0.51} photoabsorber and t-QIDE, (b) high magnification cross-sectional
52 SEM image of the device (area enclosed with red rectangle in Figure 3a), (c) back-scattered SEM
53 cross-sectional image of a finger of the device (area enclosed with red rectangle in Figure 3a).
54
55
56
57
58
59
60

1
2
3 The J - V characteristics of BC-PSCs with t-QIDEs were recorded with both front
4 (perovskite) and rear (glass) side illumination. Figure 4a shows J - V curves under 1 sun AM1.5G
5 illumination and in the dark, while relevant photovoltaic parameters are summarized in Table S4.
6
7 With front side illumination, values of 5.5 mA cm^{-2} , 0.84 V and 30% were recorded for short-
8 circuit current density (J_{SC}), open-circuit voltage (V_{OC}) and fill factor (FF), respectively, yielding
9 a PCE value of 1.4% for a reverse scan. For rear side illumination and reverse scan, a slightly
10 higher PCE value of 1.7% was obtained, with J_{SC} , V_{OC} and fill factor being 5.6 mA cm^{-2} , 0.88 V
11 and 34% , respectively. As expected, excluding CuSCN from t-QIDEs resulted in lower device
12 performance, demonstrating the advantages provided by having a hole-selective layer (Figure
13 S9). The J - V curves exhibit hysteresis, which is typically assigned to ion migration and
14 interfacial charge recombination.¹¹ The maximum power point (MPP) for the best-performing
15 device irradiated with 1 sun from the rear showed a stable output with a PCE value of *ca* 1.2%
16 maintained for at least 140 s (Figure 4b).
17
18
19
20
21
22
23
24
25
26
27
28
29
30
31
32
33
34
35
36
37
38
39
40
41
42
43
44
45
46
47
48
49
50
51
52
53
54
55
56
57
58
59
60

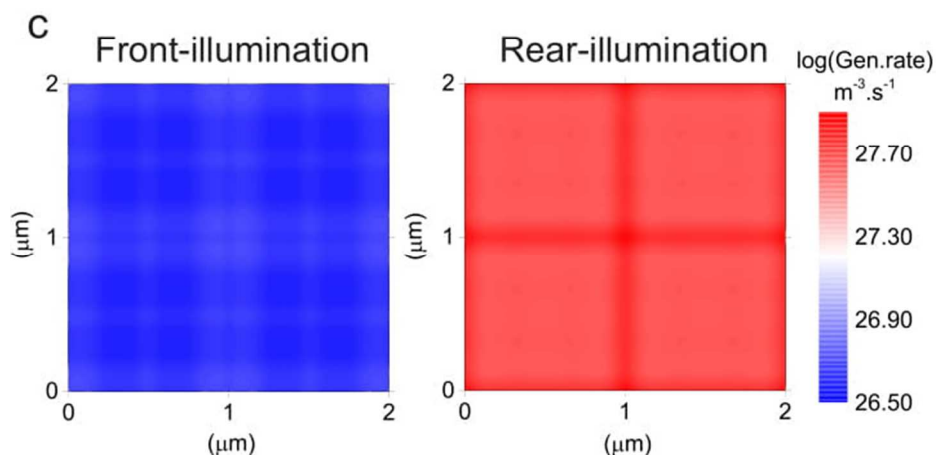
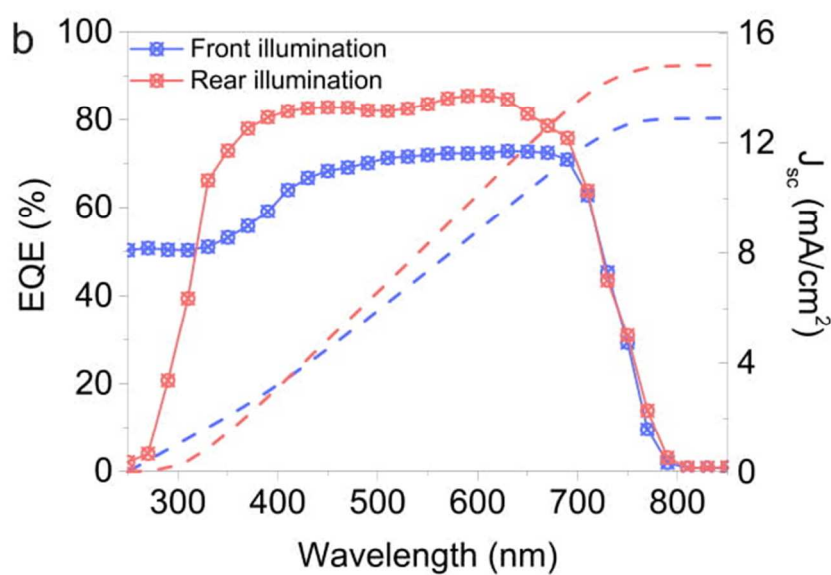
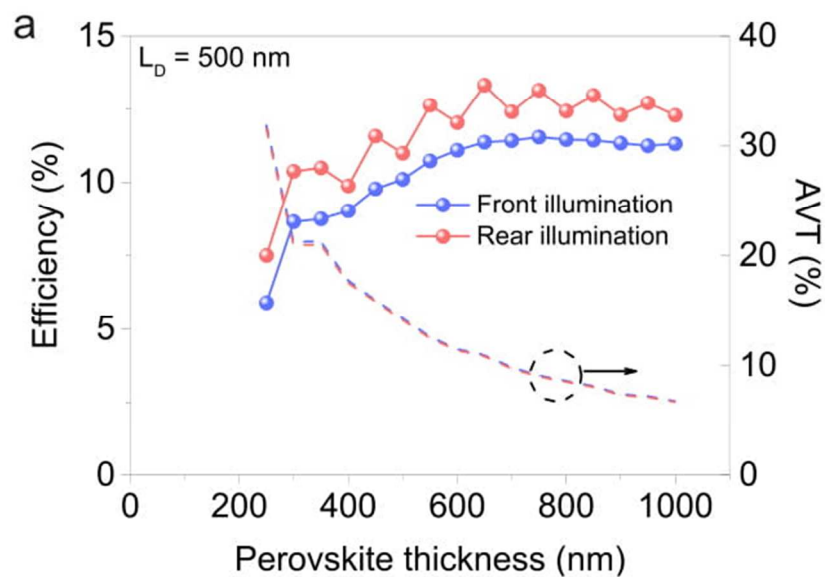


54 **Figure 4.** (a) J - V characteristics (scan rate 0.2 V s^{-1}) of a BC-PSC based on the
55 $\text{Cs}_{0.05}\text{FA}_{0.79}\text{MA}_{0.16}\text{PbI}_{2.49}\text{Br}_{0.51}$ light-absorber and a t-QIDE measured under 1 sun illumination
56
57
58
59
60

1
2
3 from the front (perovskite) side and rear (glass) side, and in the dark. (b) Evolution of
4 photocurrent and power density of the same BC-PSC at maximum power point under 1 sun
5 irradiation from the rear side.
6
7

8
9 A potential application of t-QIDEs is in semi-transparent perovskite solar cells. While the
10 PCEs of the current devices are notably below the state-of-the-art for back-contact solar cells,
11 future increases in efficiency are anticipated through increased perovskite grain sizes, a
12 decreased sheet resistance of the transparent electrodes, and improved deposition procedures for
13 the hole transport layer. To determine whether our device architecture could realistically reach
14 the PCE and average visible transmission (%AVT) of the previously reported semi-transparent
15 solar cells,¹²⁻¹³ coupled optical and electrical simulations were performed using previously
16 reported physical characteristics for key components (Table S5).²
17
18
19
20
21
22
23
24
25
26
27

28 The simulations used a realistic quality of perovskite material with a minority carrier
29 diffusion length of 500 nm. Figure 5a shows the simulated evolution of PCE as a function of
30 perovskite layer thickness with a t-QIDE with optical and electrical properties as defined in this
31 study. The simulations revealed an overall efficiency that is always higher when the cell is
32 illuminated from the glass/electrode interface (rear-illumination) vs. the air/perovskite interface
33 (front-illumination), which supports the experimental observations. A fluctuation in the PCE
34 originates from a combination of thin-film interferences and drift-diffusion carrier transport, and
35 becomes more pronounced with rear-illumination due to a higher number of modes evolved
36 passing through the multilayer structure.¹⁴ When the device is illuminated from the front or rear
37 side, the simulated maximum efficiency is *ca.* 12% (at 750 nm perovskite thickness) or *ca.* 13%
38 (at 650 nm perovskite thickness), respectively. Rear-illumination requires a ~50 nm thinner
39 perovskite layer to reach a similar efficiency to front-illumination, which also suggests more
40 efficient charge collection.
41
42
43
44
45
46
47
48
49
50
51
52
53
54
55
56
57
58
59
60



1
2
3 **Figure 5.** Simulated performance of a BC-PSC under front and rear illumination. (a) PCS and
4 AVT as a function of perovskite thickness (the perovskite thickness cannot be below the
5 thickness of the back-contact electrode, *viz.* 250 nm). (b) External quantum efficiency (EQE) at
6 the optimum thickness of the perovskite layer (750 and 650 nm for front- and rear-illumination,
7 respectively). (c) Charge generation rate of the perovskite layer in between the two back-contact
8 electrodes. The generation rate is averaged over the thickness of the perovskite and leveled to the
9 total thickness of the electrodes. The apparent interference fringes are due to optical modes
10 created by the multi layered structure evolved. Simulations were based on AM 1.5 spectrum and
11 a 500 nm minority-carrier diffusion length for the perovskite.
12
13
14
15

16
17 Figure 5a also demonstrates the potential of BC-PSCs to act as semi-transparent devices
18 when thin layers of perovskite absorber are employed. The average visible transmittance (AVT)
19 is calculated between 400 and 800 nm for comparison with reported work.¹²⁻¹³ For the thinnest
20 perovskite layer needed for the PSC to be operational, *viz.* 250 nm, which is the thickness of the
21 back-contact electrode, a potential AVT of 32% was calculated. Corresponding PCE values were
22 predicted as 5.9 and 7.5% for the devices irradiated from the front and rear, respectively (Table
23 S6). These values are comparable to previous reports for tandem organic photovoltaics.¹⁵ At the
24 maximum efficiencies, AVTs of 9.1% (front illumination, PCE = 12%) and 11% (rear
25 illumination, PCE = 13%) were calculated, demonstrating potentially superior performance.¹²⁻¹³
26
27 The back-contact architecture also permits the application of an antireflective coating, light
28 trapping, surface passivation, and photoluminescence out-coupling enhancements, which are
29 expected to improve both the PCE and AVT of an optimized device.²
30
31
32
33
34
35
36
37
38
39
40
41
42
43

44
45 To identify the contribution to charge collection efficiency across the spectrum, the
46 external quantum efficiency (EQE) of a BC-PSC at the optimal conditions for front- and rear-
47 illumination was simulated (Figure 5b). In the short wavelength range (up to 430 nm), front-
48 illumination is more efficient due to the absence of any parasitic absorption layer (ITO) in the
49 first optical path of the incoming photons. In contrast, with rear illumination, the collection
50
51
52
53
54
55
56
57
58
59
60

1
2
3 efficiency is higher within the higher wavelength range (430–780 nm), resulting in an increased
4 accumulated J_{sc} . This is partly due to better index-matching between the glass|ITO|perovskite
5 interfaces than the air|perovskite interface, effectively creating an anti-reflective coating that
6 minimizes total reflectance. This leads to increased absorption in the perovskite, and a higher
7 charge photogeneration rate near the back-contact electrode (Figure 5c). An order of magnitude
8 difference for the rear and front illumination conditions (Figure 5c) explains the experimentally
9 observed difference in J_{sc} (Figure 4a and Table S6).
10
11
12
13
14
15
16
17
18
19

20 Simulations undertaken herein suggest that further optimization of devices with t-QIDEs
21 should be possible by minimizing parasitic losses. For example, this can be achieved by
22 increasing the spacing gap size between the back-contact (for a fixed back-contact width), if
23 possible with a better quality of perovskite material (*e.g.* with minority-carrier diffusion length
24 $L_D > 10 \mu\text{m}$) (Figure S10a). Alternatively, increasing a filling fraction of the back-contact
25 electrode is seen as a promising strategy for a realistic quality of perovskite ($L_D \approx 0.5 \mu\text{m}$).
26 Unlike devices incorporating metal electrodes, the PCE is less sensitive to the width of the ITO
27 back-contact finger (Figure S10b).¹⁶
28
29
30
31
32
33
34
35
36
37
38

39 In summary, the fabrication of a transparent back-contact electrode was achieved by
40 replacing the opaque components of conventional QIDEs with ITO. These electrodes were used
41 as substrates for the first semi-transparent back-contact perovskite solar cells with a modest PCE
42 of 1.2%. Importantly, this new class of devices offers straightforward strategies for optimization
43 that could significantly increase the efficiency. Simulations showed that if these improvements
44 can be achieved, BC-PSCs incorporating t-QIDEs will offer a pathway to efficient
45 semitransparent photovoltaic devices.
46
47
48
49
50
51
52
53
54
55
56
57
58
59
60

Acknowledgements

We gratefully acknowledge the financial support from the National Science Foundation, NSF EAGER 1665279. G. D. is grateful for support from the NSF EAPSI program, OISE 1713327; E. R. thanks the Georgia Institute of Technology for support. E. R. additionally appreciates support from the Brook Byers Institute for Sustainable Systems at Georgia Tech. This work was performed in part at the Melbourne Centre for Nanofabrication (MCN) in the Victorian Node of the Australian National Fabrication Facility (ANFF). A. N. J. acknowledges an Office of the Chief Executive Postdoctoral Fellowship (CSIRO Manufacturing). Y. H. acknowledges funding from the DFG Excellence Cluster “Nanosystems Initiative Munich” (NIM), the Center for NanoScience (CeNS) and the Bavarian Collaborative Research Program “Solar Technologies Go Hybrid” (SolTech). The authors thank Mr. Mark Greaves and Dr Aaron Seeber from CSIRO Manufacturing for their help with SEM imaging and x-ray analysis, respectively. E.C.G and G.W.P.A. acknowledge financial support from the European Research Council under the European Union’s Seventh Framework Programme (FP/2007-2013)/ERC Grant Agreement 337328, “NanoEnabledPV”. The authors also acknowledge the financial support from the Australian Renewable Energy Agency (ARENA), the Australian Centre for Advanced Photovoltaics (ACAP) and the Australian Research Council through the ARC Centre of Excellence in Exciton Science (CE170100026) and project DP160104575.

Associated Content

Supporting Information available: Experimental details, materials, transparent quasi-interdigitated electrode fabrication, deposition of CuSCN layer, PV device fabrication, characterization details, details in simulation setup and device structures

References

1. Yoshikawa, K.; Kawasaki, H.; Yoshida, W.; Irie, T.; Konishi, K.; Nakano, K.; Uto, T.; Adachi, D.; Kanematsu, M.; Uzu, H., Silicon Heterojunction Solar Cell with Interdigitated Back Contacts for a Photoconversion Efficiency over 26%. *Nature Energy* **2017**, *2* (5), 17032.
2. Adhyaksa, G. W.; Johlin, E.; Garnett, E. C., Nanoscale Back Contact Perovskite Solar Cell Design for Improved Tandem Efficiency. *Nano letters* **2017**, *17* (9), 5206-5212.
3. Xiong, H.; DeLuca, G.; Rui, Y.; Li, Y.; Reichmanis, E.; Zhang, Q.; Wang, H., Solvent Vapor Annealing of Oriented PbI₂ Films for Improved Crystallization of Perovskite Films in the Air. *Solar Energy Materials and Solar Cells* **2017**, *166*, 167-175.
4. Jumabekov, A.; Della Gaspera, E.; Xu, Z.-Q.; Chesman, A.; Van Embden, J.; Bonke, S.; Bao, Q.; Vak, D.; Bach, U., Back-Contacted Hybrid Organic-Inorganic Perovskite Solar Cells. *Journal of Materials Chemistry C* **2016**, *4* (15), 3125-3130.
5. Lu, G.; Wang, J.; Qian, Z.; Shen, W., Development of Back Junction Back Contact Silicon Solar Cells based on Industrial Processes. *Progress in Photovoltaics: Research and Applications* **2017**, *25* (6), 441-451.
6. Hartnagel, H.; Dawar, A.; Jain, A.; Jagadish, C., *Semiconducting Transparent Thin Films*. Institute of Physics Bristol: 1995.
7. Helander, M.; Wang, Z.; Qiu, J.; Greiner, M.; Puzzo, D.; Liu, Z.; Lu, Z., Chlorinated Indium Tin Oxide Electrodes with High Work Function for Organic Device Compatibility. *Science* **2011**, *332* (6032), 944-947.
8. Yan, L.; Schropp, R., Changes in the Structural and Electrical Properties of Vacuum Post-Annealed Tungsten-and Titanium-Doped Indium Oxide Films Deposited by Radio Frequency Magnetron Sputtering. *Thin Solid Films* **2012**, *520* (6), 2096-2101.
9. Gupta, R.; Ghosh, K.; Mishra, S.; Kahol, P., High Mobility W-Doped In₂O₃ Thin Films: Effect of Growth Temperature and Oxygen Pressure on Structural, Electrical and Optical Properties. *Applied Surface Science* **2008**, *254* (6), 1661-1665.
10. Saliba, M.; Matsui, T.; Seo, J.-Y.; Domanski, K.; Correa-Baena, J.-P.; Nazeeruddin, M. K.; Zakeeruddin, S. M.; Tress, W.; Abate, A.; Hagfeldt, A., Cesium-Containing Triple Cation Perovskite Solar Cells: Improved Stability, Reproducibility and High Efficiency. *Energy & Environmental Science* **2016**, *9* (6), 1989-1997.
11. Calado, P.; Telford, A. M.; Bryant, D.; Li, X.; Nelson, J.; O'Regan, B. C.; Barnes, P. R., Evidence for Ion Migration in Hybrid Perovskite Solar Cells with Minimal Hysteresis. *Nature Communications* **2016**, *7*, 13831.
12. Roldan-Carmona, C.; Malinkiewicz, O.; Betancur, R.; Longo, G.; Momblona, C.; Jaramillo, F.; Camacho, L.; Bolink, H. J., High Efficiency Single-Junction Semitransparent Perovskite Solar Cells. *Energy & Environmental Science* **2014**, *7* (9), 2968-2973.
13. Della Gaspera, E.; Peng, Y.; Hou, Q.; Spiccia, L.; Bach, U.; Jasieniak, J. J.; Cheng, Y.-B., Ultra-Thin High Efficiency Semitransparent Perovskite Solar Cells. *Nano Energy* **2015**, *13*, 249-257.
14. Brongersma, M. L.; Cui, Y.; Fan, S., Light Management for Photovoltaics using High-Index Nanostructures. *Nature materials* **2014**, *13* (5), 451.
15. Chen, C.-C.; Dou, L.; Gao, J.; Chang, W.-H.; Li, G.; Yang, Y., High-Performance Semi-Transparent Polymer Solar Cells Possessing Tandem Structures. *Energy & Environmental Science* **2013**, *6* (9), 2714-2720.

1
2
3 16. Knight, M. W.; Van De Groep, J.; Bronsveld, P. C.; Sinke, W. C.; Polman, A., Soft
4 Imprinted Ag Nanowire Hybrid Electrodes on Silicon Heterojunction Solar Cells. *Nano Energy*
5 **2016**, *30*, 398-406.
6
7
8
9
10
11
12
13
14
15
16
17
18
19
20
21
22
23
24
25
26
27
28
29
30
31
32
33
34
35
36
37
38
39
40
41
42
43
44
45
46
47
48
49
50
51
52
53
54
55
56
57
58
59
60